Accommodation coefficient investigation in rectangular microchannels for large Knudsen number range

M. Hadj-Nacer, I. Graur, P. Perrier

Université de Provence- Ecole Polytechnique Universitaire de Marseille,
Département de Mécanique Energétique, UMR CNRS 6595, 5 rue Enrico Fermi,
13453 Marseille cedex 13, France
mustafa.hadjnacer@polytech.univ-mrs.fr, irina.graour@polytech.univ-mrs.fr,
pierre.perrier@polytech.univ-mrs.fr

ABSTRACT

Experimental investigations on the tangential moment accommodation coefficient (TMAC) in two rectangular microchannels covered with a layer of Gold (Au) and of Silica (SiO_2) on the internal surfaces is presented. Both microchannels have very smooth internal surfaces with mean roughness close to $1nm$ and similar aspect ratios. The experimental technique 'Constant Volume Method' is used to measure the mass flow rate through these microchannels for three gases (He, N_2 and Ar). A wide Knudsen number interval $(0.02 - 10)$ ranging from the hydrodynamic to the near free molecular regimes is examined in this study. The continuum approach associated to the first order velocity slip boundary condition was used in the slip regime. In the transitional and near free molecular regimes numerical calculations of the mass flow rate using the linearized kinetic BGK model equation are performed. These numerical results are compared with the measured values of the mass flow rate and the TMAC is extracted.

Keywords: Gas flow, mass flow rate, pressure measurement, TMAC.

1 INTRODUCTION

The gas-solid interaction at microscale was one of the main studies for which the scientists demonstrated a significant interest. Many experimental investigations have been carried out in the last years to study the flow interaction with wall [1],[2], [3], [4],[5]. At microscopic level this interaction is essentially characterized by the tangential momentum accommodation coefficient (TMAC) which describes the way of the gas-wall exchange accompanying the reflection on the wall. The main experimental techniques used to measure the TMAC for different surfaces and gases were reviewed in [6]. This review shows that the TMAC depends on a number of parameters such as the nature of the gas, the surface material, its cleanliness and its roughness.

Two main experimental techniques are widely used for the mass flow rate measurements in microchannels. The first one is the liquid drop method ([3], [4], [5], [7],[8],[9]) and the second one is the constant volume technique ([3] [7], [10], [11]). Both techniques were realized for isothermal flow conditions. The Knudsen number range investigated in these studies were limited essentially to the slip flow regime. The TMAC is deduced from the measurements of the mass flow rate by comparing the measured values with the continuum and kinetic models and it is found in the range $(0.8 - 1)$ [7], [10], [11], [12].

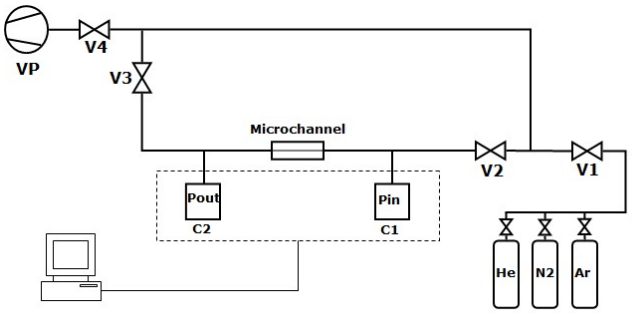

Figure 1: Experimental setup

The aim of this paper is an experimental study of the interaction between various gases and two different materials surfaces (Gold and Silica) with low roughness. The isothermal mass flow rate through two microchannels coated on their internal surfaces by gold and silica layers is measured using the constant volume technique. The slip and accommodation coefficients are deduced by using the experimental data of the mass flow rate and the Navier-Stokes model with the slip boundary conditions in the slip regime. In the transitional and the near free molecular regimes, the linearized BGK kinetic model are fulfilled and the experimental results are compared with the numerical calculations.

2 EXPERIMENTS

The experimental setup is represented schematically in Fig. 1. The mass flow rate of three gases (He, N_2 and Ar) through the rectangular microchannels is measured using the constant volume technique. This technique involve the use of two constant volume tanks connected by a microchannel. The volume of the tanks has to be much greater than the microchannel volume to guarantee that the flow parameters are independent of time, but remain detectable. The pressure and temperature variation during the experiments are measured and the

Table 1: Microchannels dimensions and surfaces roughness

Microchannel	H $\times 10^6$ [m]	W $\times 10^6$ [m]	L $\times 10^3$ [m]	Ra $\times 10^9$ [m]
G	27.84 ± 0.5	52.23 ± 0.5	15.07 ± 0.01	0.87 ± 0.02
S	24.30 ± 0.5	50.10 ± 0.5	13.68 ± 0.01	1.12 ± 0.02

mass flow rate is deduced from the equation of state. The mass variations occurring in the tanks during the experiments do not call into question the stationary assumption because the pressure variations are maintained less than 2% during the measurements. The registration of the pressure variation in the inlet and outlet tanks is carried out using two pressure transducers C1 and C2 (see Fig. 1) chosen according to their pressure range and connected to the upstream and downstream tanks, respectively. The temperature of the gas in the system is assumed to be equal to the room temperature. The thermal stabilization is checked before and during each experiment.

The rectangular microchannels used in the experiments are etched in two silicon wafer according to a cavity of $H/2$ depth. Then a layer of Gold or Silica is deposed and the two wafers are assembled using a gold-gold bonding. The dimensions of the microchannels (H: Height, W: Width, L: Length) are measured using optical microscope and are given in Tab. 1 with the mean value of the surface roughness (Ra). It is to be noted that the channel aspect ratios H/W are slightly different and are equal to 0.533 and 0.485 for the channel covered by gold and silica, respectively. In this article, we refer with letter G and S to the microchannels with Gold (Au) and Silica(SiO_2) deposit, respectively.

3 MASS FLOW RATE

Using the constant volume technique, the mass flow rate can be calculated from the equation of state for ideal gas

$$pV = mRT, \tag{1}$$

where V represents the tank volume and R is the specific gas constant. p, T and m are, respectively, the pressure, temperature and mass of the gas. For small variation of the gas pressure, mass and temperature equation (1) can be transformed into

$$\frac{dm}{dt} = \frac{d}{dt}\left(\frac{pV}{RT}\right). \tag{2}$$

As it was shown in [1], [7], the previous relation may be written as follows

$$\frac{dm}{dt} = \frac{V}{RT}\frac{dp}{dt}(1-\varepsilon), \qquad \varepsilon = \frac{dT/T}{dp/p}. \tag{3}$$

If ε is small compared to 1, then dm/dt can be considered as the mass flow rate Q_m through the microchannel. The constant volume method requires a high-thermal stability. The deviation of the temperature from the initial value is smaller than $0.5K$. The relative variation of the temperature dT/T is in order of 2×10^{-4} against 10^{-2} for the relative variation of the pressure dp/p, ε is clearly less than 2×10^{-2}. Thus, the mass flow rate Q_m can be written under the following form

$$Q_m = \frac{V}{RT}\frac{\delta p}{\tau}. \tag{4}$$

The measurement of Q_m is affected by a specific relative error of 2×10^{-2} due to the temperature variation. To determine the mass flow rate we use the registered data of the pressure p_i at different instants t_i. The stationary assumption can justify physically the implementation of first order polynomial expression in t_i

$$p(t_i) = at_i + b, \qquad a = \frac{\delta p}{\tau}. \tag{5}$$

To determine the coefficients a and b, we used the least squares method. The uncertainty on the coefficient a is calculated from standard deviation following the method used in [7] and its value is less than 0.5%. Therefore, the uncertainty on the measurement of the mass flow rate is calculated from

$$\frac{\Delta Q_m}{Q_m} = \frac{\Delta V}{V} + \frac{\Delta T}{T} + \frac{\Delta a}{a} \tag{6}$$

and is less than ±4.1% ($\Delta V/V = \pm 1.6\%$, $\Delta T/T = \pm 2\%$, $\Delta a/a = 0.5\%$).

3.1 RESULTS AND DISCUSSION

Due to the large Knudsen number range $(0.002 - 10)$ investigated in this study we split it in two parts. First, for $Kn_m \leq 0.1$ we used the continuum Navier Stokes model with the first order slip boundary condition. Second, for $Kn_m > 0.1$ we performed numerical simulation of the mass flow rate using the linearized BGK model assuming specular-diffuse accommodation of the molecules at the wall.

3.2 Hydrodynamic and slip regimes

In order to estimate the velocity slip coefficients the measured mass flow rate was fitted with a first order polynomial form of Kn_m by using the least square method detailed in [4].

$$S^{exp} = 1 + A^{exp} Kn_m, \tag{7}$$

Table 2: Experimental A^{exp}, slip and accommodation coefficients

	G			S		
Gas	A^{exp}	σ_p	α	A^{exp}	σ_p	α
He	9.741±0.131	1.305±0.019	0.868±0.007	8.039±0.044	1.091±0.007	0.962±0.003
N_2	10.178±0.083	1.364±0.012	0.845±0.004	8.273±0.046	1.123±0.007	0.947±0.003
Ar	10.017±0.126	1.342±0.019	0.853±0.007	8.413±0.073	1.142±0.011	0.938±0.005

The coefficient A^{exp} is obtained by applying the non-linear square Marquard-Levenberg algorithm to the measured values of the mass flow rate. The uncertainty on this coefficient was estimated using the standard error. The "experimental" slip coefficient σ_p can be deduced from the comparison of the theoretical and experimental normalized mass flow rate. Further explanations can be found in the reference [10]. When the slip coefficient is known the TMAC may be calculated. The method used to calculate the TMAC is proposed in [13] taking into account the Knudsen layer influence. A simple expression associating the slip coefficient and the TMAC is proposed

$$\sigma_p(\alpha) = \frac{2-\alpha}{\alpha}(\sigma_p(1) - 0.1211(1-\alpha)), \qquad (8)$$

where $\sigma_p(1)$ the slip coefficient for $\alpha = 1$ equals 1.016 [14]. The TMAC calculated from the slip coefficient using (8) are given in Tab. 2.

The experimental coefficients A^{exp} obtained for both microchannels G and S and for the gases He, N_2 and Ar are shown in Tab. 2. The determination coefficient r^2 and the residual variance s_r are calculated but not presented here. The values of r^2 are very close to 1 (the lower value is 0.993) which confirms the quality of fitting for both microchannels. Whereas, the residual variance s_r is smaller for the microchannel S than G.

The experimental estimations of the velocity slip coefficient are given in Tab. 2. These values are calculated using the first order fitting for the Knudsen number range $[0-0.1]$. The errors in Tab. 2 derive from the experimental error in A^{exp} and do not take into account the systematic uncertainty coming from the errors on the mass flow rate measurements, see (6) and the errors due to the channel dimension measurements.

The values of the slip coefficient are different from those obtained theoretically in [15] ($\sigma_p = 1.012$) and in [14] ($\sigma_p = 1.016$) using the BGK kinetic model with assumption of full accommodation of the molecule at the wall, as the accommodation is not complete in our experimental conditions.

The roughness effect on the gas-solid interaction can not be deduced from this study as the both surfaces of the microchannels are quiet smooth, they have a mean roughness around the value $1nm$. While, the material surfaces influence on the interaction gas-solid is well notifiable by the comparison between the results of the TMAC for the microchannels (see Tab. 2). The values of TMAC obtained for Silica surface material are significantly larger than those obtained for the Gold surface material.

For the gold surface channel the difference between the higher and lower values of the TMAC in Tab. 2 is less than 2.6%, less than experimental uncertainties. That probably means that the gas type has no significant effect on the interaction gas-solid gold, when the surfaces of the microchannel are very smooth (relative roughness of 0.0031%). For the silica surface channel, as previously said, the TMACs are larger, the differences according to the gases are more significant and the hierarchy according to the molecular mass may be observed.

The TMAC values obtained in this study confirm the non complete accommodation of the molecule at the wall. The TMACs lie in the range $0.84 - 0.97$. The values obtained for the silica surface are always higher then those of the gold surface.

3.3 Transitional and free molecular regimes

The transitional and near free molecular regimes are the most complicated regimes from theoretical and experimental point of view. In this regimes the rarefaction increases and the detection of the flow parameters, especially, the variation of the pressure in the tanks becomes difficult and require a very high sensitive pressure transducer. At lowest value of the pressure in the outlet tank the variation of the pressure in this tank is about $0.284Pa$ during the experimental time length $\tau = 250s$ which means that the variation per second is equal to $1.1 \times 10^{-3} Pa/s$. In our experiments we use a very high sensitive pressure transducer that have a resolution of 1.5×10^{-5} of full scale and accuracy of 0.2%.

The measured values of the mass flow rate in the transitional and near free molecular regimes are presented in Fig. 2 in non-dimensional form according to following expression

$$G = \frac{L\sqrt{2RT}}{H^2 W(p_{in} - p_{out})}\dot{M} \qquad (9)$$

for both microchannels G and S and for the working

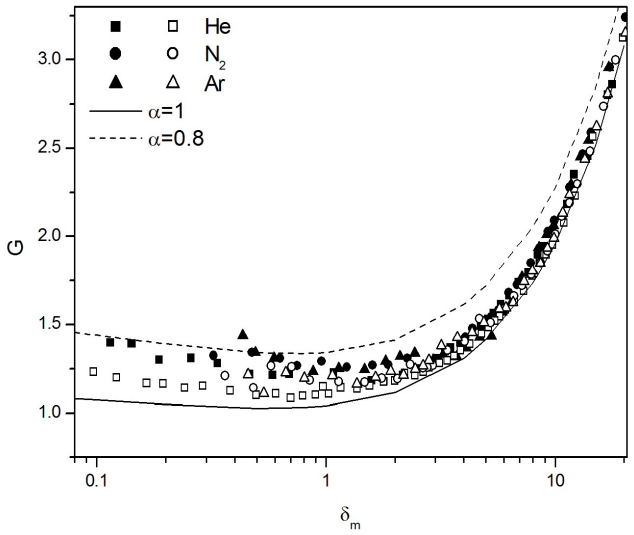

Figure 2: Dimensionless mass flow rate. Experimental points vs theoretical lines. Filled and non-filled symbols are for microchannel G and S, respectively

gases He, N_2 and Ar. The results were plotted as function of the rarefaction parameter δ_m which is calculated from the mean pressure of the two tanks. The solution of the linearized BGK equation for two values of the TMAC (0.8 and 1.0) are obtained numerically for the aspect ratio $H/W = 0.5$ and the results are plotted in Fig. 2.

From visual comparison of the experimental and the theoretical curves, it is well noticed that the values of the TMAC for both microchannels are less than 1.0, and are in the range $0.8 - 1.0$ for all gases. For the gold covered microchannel the value of α appear close to 0.9. The values of the mass flow rate obtained for the microchannel G are always larger than those obtained for the microchannel S, the difference is small for $\delta_m > 2$ and becomes more significant when δ_m is less than 2. Conversely the TMAC is larger with S then with G. Globally, the results observed confirm those obtained in slip regime: incomplete accommodation at the wall, more important accommodation on the silica wall than on the gold wall. Presently the numerical curves are drown for unique aspect ratio equal to 0.5: we have to differentiate the calculation for each channel (0.533 for the gold channel and 0.485 for the silicon channel).

4 CONCLUSION

Experimental and numerical investigations on the flow through rectangular microchannels are presented. The constant volume technique was used to measure the mass flow rate of three gases (He, N_2 and Ar) through rectangular microchannels. To obtain the TMAC the continuum approach was used in the slip regime with first order boundary condition, whereas in the transitional regime the linearized BGK kinetic model was used.

The effect of the materials surface on the interaction gas-solid was highlighted by comparing the values of the TMACs of two surface materials (Gold and Silica). The gold coat gives a more specular reflection and tends to make insignificant the influence of the gas interacting at the wall.

Acknowledgements

The research leading to these results has received funding from the European Community's Seventh Framework Programme (ITN - FP7/2007-2013) under grant agreement n°215504.

Acknowledgment to Femto-ST (Besançon-France) for providing the microchannels.

REFERENCES

[1] Arkilic, E. B., Breuer, K. S., and Schmidt, M. A. *Journal of fluid mechanics* **437**, 29–43 (2001).

[2] Arkilic, E. B., Schmidt, M. A., and Breuer, K. S. *Journal Microelectomech Systeme* **6**(2), 167–178 (1997).

[3] Colin, S., Lalonde, P., and Caen, R. *Heat Transf Eng* **25**(3), 23–30 (2004).

[4] Maurer, J., Tabeling, P., Joseph, P., and Willaime, H. *Phys. Fluids* **15**, 2613–2621 (2003).

[5] Zohar, Y., Lee, S. Y. K., Lee, W. Y., Jiang, L., and Tong, P. *Fluid Mechanics* **472** (2011).

[6] Agrawal, A. and Prabhu, S. V. *Journal of Vac. Sci. Technol.* **4**(26) (2008).

[7] Ewart, T., Perrier, P., Graur, I. A., and Méolans, J. G. *Experiments in Fluids* **41**(3), 487–498 (2006).

[8] Harley, J., Huang, Y., Bau, H., and Zemel, J. *Fluid Mechanic* **284**, 257–274 (1995).

[9] Lalonde, P. PhD thesis, Institut National des Sciences Appliqueés de Toulouse, France, (2001).

[10] Ewart, T., Perrier, P., Graur, I. A., and Méolans, J. G. *Journal of fluid mechanics* **584**, 337–356 (2007).

[11] Pitakarnnop, J., Varoutis, S., Valougeorgis, D., Geoffroy, S., Baldas, L., and Colin, S. *Microfluid and Nanofluid* **8**, 57–72 (2010).

[12] Porodnov, B. T., Suetin, P. E., Borisov, S. F., and Akinshin, V. D. *J. Fluid Mech.* **64**(3), 417–437 (1974).

[13] Loyalka, S. K., Petrellis, N., and Stvorick, S. T. *Phys. Fluids* **18**, 1094 (1975).

[14] Cercignani, C. and Daneri, A. *Phys. Fliuds* **6**, 993–996 (1963).

[15] Kogan, M. N. Plenum Press New York, (1969).